

BEHAVIORS OF THERMOELASTIC PROPERTIES IN NI-TI-BASED SHAPE MEMORY ALLOYS, PROCESSED BY METAL FORMING TECHNIQUES

TARSILA TENÓRIO LUNA DA SILVA^{1*}, FILLIPE VIRGOLINO², NIÉDSON SILVA³,
CARLOS OLIVEIRA⁴, CARLOS ARAÚJO⁵, OSCAR OLIMPIO DE ARAUJO FILHO⁴
AND CEZAR GONZALEZ⁴

¹*Departamento de Engenharia Mecânica (DEM),
Universidade Federal da Bahia (UFBA), Salvador, Brazil*

²*Departamento de Engenharia Mecânica (DEMEC),
Universidade de Pernambuco (UPE), Recife, Brazil*

³*Departamento de Engenharia Mecânica (DEMEC),
Instituto Federal de Pernambuco (IFPE), Caruaru, Brazil*

⁴*Departamento de Engenharia Mecânica (DEMEC),
Universidade Federal de Pernambuco (UFPE), Recife, Brazil*

⁵*Departamento de Engenharia Mecânica (DEMEC),
Universidade Federal de Campina Grande (UFCG), Campina Grande, Brazil*

*Corresponding author: tarsila.silva@ufpe.br

(Received: 14 May 2022; Accepted: 23 March 2023; Published on-line: 4 July 2023)

ABSTRACT: In this work, the thermoelastic properties of Ni-Ti shape memory alloys (SMA) processed by conventional rolling and equal channel angular extrusion (ECAE) were investigated. SMAs have two phases: Austenite (at high temperature) and Martensite (at low temperature). The samples were compared under five different thermal and processing conditions: homogenized, rolled, rolled-annealed, extruded, and extruded-annealed. The homogenized sample served as a reference. The samples were analyzed by differential scanning calorimetry (DSC) to determine the thermoelastic transformation temperatures. Images were taken using scanning electronic microscopy (SEM) in conjunction with energy dispersive spectroscopy (EDS). The dynamic area was completed for two tests: under constant load bending (simulation of the memory effect to determine the reversible thermoelastic strain) and dynamic mechanical analysis (DMA). The results showed that the plastic forming processes alter the properties, especially for samples exposed to the ECAE, which can block the martensitic phase. However, R-phase (a rhombohedral phase), that can appear at low temperatures before the martensitic phase, emerges totally when the extruded sample suffers annealing. The images of SEM, confirmed by EDS, show that any type of forming process and the presence of precipitates have a significant influence on the behavior of the elastic property. It was found that extrusion has a greater effect on the restoring properties of the alloys than rolling. This analysis is of great importance for the use of SMA in applications requiring high mechanical strength combined with the functional properties of shape recovery through martensitic phase transformations.

ABSTRAK: Kajian ini adalah berkaitan sifat-sifat bentuk aloi ingatan (SMA) termoelektik Ni-Ti yang diproses melalui pengelekan konvensional dan penyemperitan sudut saluran sama (ECAE). SMA mempunyai dua peringkat: Austenit (pada suhu tinggi) dan Martensit (pada suhu rendah). Sampel dibandingkan pada lima tahap kepanasan dan proses iaitu: percampuran, penggulangan, penggulangan-rataan, perataan dan penyemperitan-rataan. Sampel campuran yang dihomogenkan dijadikan sebagai sampel rujukan. Sampel dianalisis dengan pengimbas kalorimetri pembezaan (DSC) bagi menentukan suhu

transformasi termoeplastik. Imej diambil menggunakan pengimbas mikroskop elektronik (SEM) bersama spektroskopi penyebaran tenaga (EDS). Kawasan dinamik diuji dengan dua ujian: di bawah lenturan beban malar (simulasi kesan memori bagi menentukan terikan termoeplastik boleh balik) dan analisis mekanik dinamik (DMA). Dapatan kajian menunjukkan bahawa proses pembentukan plastik telah mengubah sifat, terutama pada sampel yang terdedah kepada penyempitan sudut saluran sama ECAE, yang boleh menyekat fasa martensit. Walau bagaimanapun, fasa-R (fasa rombohedral) yang boleh muncul pada suhu rendah sebelum fasa martensitik, muncul sepenuhnya apabila sampel tersempit mengalami penyepuhhindapan (penyempitan-rataan). Imej pengimbasan mikroskop elektronik, seperti yang dibuktikan dengan spektroskopi penyebaran tenaga (EDS), menunjukkan bahawa apa-apa jenis proses pembentukan dan kehadiran mendakan mempunyai pengaruh kuat terhadap sifat elastik. Dapatan kajian juga mendapati bahawa penyempitan mempunyai kesan yang lebih besar terhadap sifat pemulihan aloi berbanding proses penggulungan. Analisis ini sangat penting bagi penggunaan bentuk aloi ingatan (SMA) dalam aplikasi yang memerlukan kekuatan mekanikal yang tinggi bersama sifat pemulihan bentuk melalui transformasi fasa martensit.

KEY WORDS: *equal channel angular extrusion; shape memory alloy; Ni-Ti alloys*

1. INTRODUCTION

Shape memory alloys (SMA) are active materials that can restore plastic deformations through suitable thermal conditioning. The phenomenon of shape memory effect (SME) is closely related to martensitic phase transformations, which are crystallographically reversible [1]. Figure 1 summarizes the shape memory effect when comparing an ordinary plastic deformation, a superelastic deformation and a shape memory deformation.

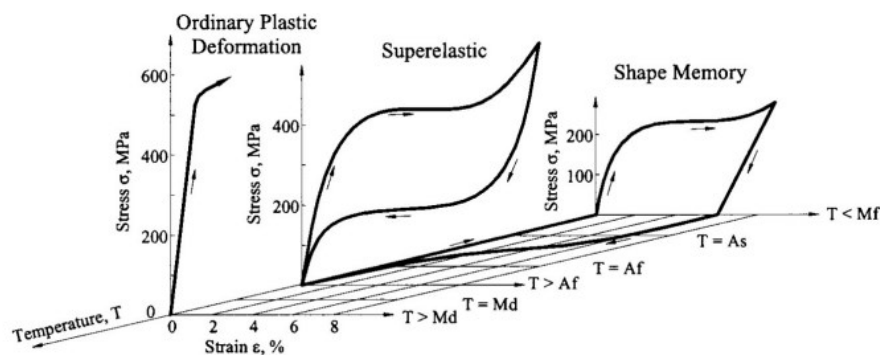


Fig. 1: Comparison between the diagram "stress x strain" in 3 forms: ordinary plastic deformation, superelastic deformation and deformation with shape memory [2] *apud* [3].

SMAs have two phases: Austenite (at high temperature) and Martensite (at low temperature). The phase transformation temperatures are austenite onset (As), austenite end (Af), martensite onset (Ms), martensite end (Mf) and martensite transformation temperature by deformation (Md). Figure 1 shows that superelastic and shape memory deformations can be as high as 8%. The SMAs can also deform with a temperature difference [2]. The fabrication of Ni-Ti family SMAs is of great importance because slight variations in chemical composition can change the critical temperatures of martensitic transformation to about 100 °C [2]. Therefore, plasma is efficiently used for the manufacturing process as it leads to negligible losses due to oxidation during melting [4]. Ni-Ti based SMAs are widely used due to their wide range of technological applications, ranging from aerospace and biomedical to petrochemical and other industries [5,6].

The SMA can be considered an electric drive if the SME is activated by the application of current pulses (Joule effect). On the other hand, if the SME is activated directly by controlled temperature changes, they are considered thermal actuators. When these alloys are subjected to plastic deformation processes, they exhibit increased mechanical strength due to their hardening (significant increase in the density of crystalline defects) and reduced grain size after deformation and heat treatment. This change in mechanical properties leads to changes in the thermoelastic properties of SMA (critical transformation temperatures, transformation enthalpies, thermoelastic deformation, thermal hysteresis and others), which are essential characteristics for the use of these materials in technological applications [7,8].

Equal channel angular extrusion (ECAE) or equal channel angular pressing (ECAP) is a metal-forming process recently developed by Segal et al. [9]. The process promotes the passage of material between two successive channels that intersect, forming angles between 90° and 120° and causing plastic deformation. These channels have identical geometric dimensions so that material does not change its dimensions after processing. In this process, the material undergoes several plastic deformations that cause high critical shear stress without changing the cross-section of the sample. Some studies show that the deformation phenomena during the ECAE process are independent of the sample size [6]. Several technological applications of these processed materials are already idealized, especially for parts that need to have a high mechanical strength obtained by plastic deformation processes without changing their dimensions during processing.

Sun et al. [10] examined the properties and hardening behavior of ECAE-processed Mg-Al binary alloys. As a result, the dynamic compressive test shows a significant strength increase attributed to the precipitates and the strength improvement from grain size refinement (Hall-Petch effect). Yang et al. [11] processed Ni-Ti-Nb SMAs by ECAP. Ni-Ti-Nb is a wide hysteresis shape memory alloy with great application potential in aerospace. The ECAP process decreased grain size (or the increase of grain boundary content), and the transformation hysteresis temperature and recovery stress of the Ni-Ti-Nb alloy increased simultaneously. Ni-Ti shape memory alloys are widely used for medical components, as they can accommodate large strains in their superelastic state. To further improve the mechanical properties of Ni-Ti, grain refinement by severe plastic deformation is applied to generate an ultrafine-grained microstructure with increased strength. Leitner et al. [12] performed experiments in ultrafine-grained Ni-Ti, processed by ECAP, and comprehensive fracture and fatigue crack growth experiments to assess its damage tolerance, which is essential for safely using this material in medical applications.

Other methods of plastic forming were studied. Jiang et al. [13] studied the mechanically induced martensite in Ni-Ti-Fe alloys, with shape memory effect, manifesting the suggested in the deformation plane, concluding that the plastic deformation necessary to produce the product of the dislocations plays an essential role in the formation of mechanically induced martensitic transformation, unlike stress-induced martensite where control of dislocations only occurs after deformation. Zhang et al. [14] subjected Ni-Ti-based superelastic alloys to severe cold rolling and observed that stress-induced martensite reorientation (B19' phase) dominates the reaction. Liang et al. [15] described the martensitic strain states of cold-rolled Ti50.8at%Ni alloys for different thickness reduction levels. Silva [16] rolled two Ni-Ti wires with a shape memory effect. Both wires showed important characteristics and high performance, such as good responses to several cold rolling, low thermal hysteresis, reasonable dimensional control, nanostructure, and excellent properties mechanics. It can be used in highly complex engineering applications requiring precision in actuation and control.

This study aims to obtain a Ni-Ti alloy with an SME and subject these materials to mechanical forming processes by conventional rolling and ECAE. In the work, the properties of Ni-Ti SMA were analyzed using DSC analysis, SEM-EDS and a constant bending load test. The latter test simulates the shape memory effect and the thermoelastic properties are determined from the curves obtained.

2. MATERIALS AND METHODS

A SMA of the equiatomic composition of Ni-50at.%Ti, corresponding to Ni-45wt.%Ti, was obtained by the plasma skull-push pull (PSPP) process with a controlled atmosphere melting chamber. A plasma flame of a tungsten electrode melts the metallic material. Plasma energy is enough for melting most metallic alloys cleanly and efficiently. The furnace chamber receives high pressure by vacuum in its mold cavity, continuously filling the mold in a push-pull sequence. The machine has a mode control that determines time and temperature according to the alloy [17,18]. It was found that to ensure good homogeneity of the SMA, the melting process should be repeated five times. Heat treatments were made in a Jung muffle furnace, model LF4212, followed by cooling in water. The ingot was homogenized for 120 min in a muffle furnace at 900 °C, followed by quenching in water at room temperature (~25 °C).

The ingot was cut on a precision cutter with a diamond disk to produce samples as prismatic bars for metal forming processes: conventional mechanical rolling process and ECAE. The sample used in the rolling process has $5 \times 1.5 \text{ mm}^2$. Hot rolling was performed on a conventional rolling machine. After each step, the sample was heated in a muffle furnace at 900 °C for 1 min. The sample was deformed from 1.5 mm to 0.5 mm, with a final deformation rate of 66.7% (20 steps with 0.05 mm for each step). For the angular extrusion, the sample was a bar with a $5 \times 5 \text{ mm}^2$ square cross-section. The die for the angular extrusion process has an angle of 130° between internal channels. Angular extrusion was performed on a universal mechanical testing machine (EMIC), controlled to operate in a compression test mode with $0.5 \text{ mm} \cdot \text{min}^{-1}$ speed at room temperature (~25 °C).

This work obtained samples after homogenization (using a sample without plastic deformation as a reference), mechanical rolling, and ECAE. The samples obtained for each plastic deformation process were subjected to annealing at 450 °C for 15 min and cooled in water at room temperature for stress relief. Table 1 presents the nomenclature and procedures applied to each of the samples analyzed in this study.

Table 1: Nomenclature and procedures of the Ni-Ti samples

Sample	Processes applied
H	Homogenized at 900 °C for 120 min
RL	Rolled
RA	Rolled and annealed at 450 °C for 15 min
E	Extruded
EA	Extruded and annealed at 450 °C for 15 min

The calorimetric properties (temperatures and enthalpies of austenitic, martensitic, and rhombohedral phase transformations and their thermal hysteresis) were performed by a Mettler TA3000 DSC. The DSC technique is very effective for determining the record of phase transformation temperatures in LMF. The advantage of this technique is the possibility of measuring the energy involved in the process based on measuring the area of

the endothermic peak in heating and the exothermic peak in cooling. Even so, the transformation enthalpies, thermal hysteresis (difference between the transformation peak temperatures), and phase transformation temperatures (A_s , A_f , M_s , M_f measured by crossing the tangents at the peaks) are measured. This technique also allows obtaining graphs, in which it is possible to analyze whether the phase transformation occurs in one or two steps [19,20]. The DSC heating chamber was filled with nitrogen gas to prevent the oxidation of the material. The samples were analyzed over a temperature range of $-60\text{ }^\circ\text{C}$ to $120\text{ }^\circ\text{C}$, with a heating/cooling rate of $10\text{ }^\circ\text{C}/\text{min}$.

The DMA experiment consisted of applying an oscillating force to a sample in uniaxial tension mode and investigating the response of the material to this applied load. The equipment allows working between $25\text{ }^\circ\text{C}$ and $500\text{ }^\circ\text{C}$ in bending, tensile and uniaxial cantilever (curved at one end and free at the other) modes [21,22].

In this work, DMA tests were performed on equipment installed in an anti-vibration bed to avoid interference during data acquisition. The experiment was conducted in single cantilever mode, following standard parameters: frequency of 1 Hz, a heating rate of $2\text{ }^\circ\text{C}/\text{min}$ and a vibration amplitude of $5 \times 10^{-3}\text{ mm}$ [23]. The SMA Ni-Ti slides used had a useful length and width of approximately 17 and 5 mm, respectively. Prior to all tests, the samples were cooled to temperatures of about $-30\text{ }^\circ\text{C}$ to collect data on the reverse martensitic transformation upon heating. As with the DSC tests, the transformation temperatures obtained from the DMA curves were determined using the tangent crossing method. Conventional metallographic procedures (grinding and polishing with diamond paste) were performed and Kroll reagent (2 mL HF, 4 mL HNO_3 , and 100 mL H_2O) was used for etching. The microstructures of the samples were recorded with a Hitachi TM3000 SEM. Together with the SEM-EDS tests are carried out to semi-quantitatively check the chemical composition of the sample.

A special apparatus was developed to determine the thermoelastic properties of SMA under constant bending load (cantilever test). The load is applied to the sample through a pulley system. A programmable silicon oil bath is used to perform heating and cooling cycles between $-10\text{ }^\circ\text{C}$ and $100\text{ }^\circ\text{C}$. During cooling, the plate (sample) is deformed, and when heated, the sample regains its original shape. A Linear Variable Displacement Transducer (LVDT) and a thermocouple measure the deformation and temperature, respectively [24].

In this work, the samples were individually tested under a constant bending load of 80 MPa and thermally cycled 20 times between $20\text{ }^\circ\text{C}$ and $100\text{ }^\circ\text{C}$ with a rate of $10\text{ }^\circ\text{C}\cdot\text{min}^{-1}$ during heating and $3\text{ }^\circ\text{C}\cdot\text{min}^{-1}$ for cooling. The samples have prismatic bar geometry with dimensions of $20 \times 5 \times 0.5\text{ mm}^3$.

Figure 2 shows representative thermoelastic deformation versus temperature curves obtained from data collected in the thermomechanical tests under constant load. There are two cycles, in which thermoelastic properties are determined. The martensitic transformation temperatures (austenite and martensite phases) can be found across the tangent line technique. Thermoelastic deformations (ϵ_t) and previous plastic strain (x) are found in the ordinate axes as indicated in Fig. 2. The thermal hysteresis ($H_t = A_{50} - M_{50}$) can be also calculated [25].

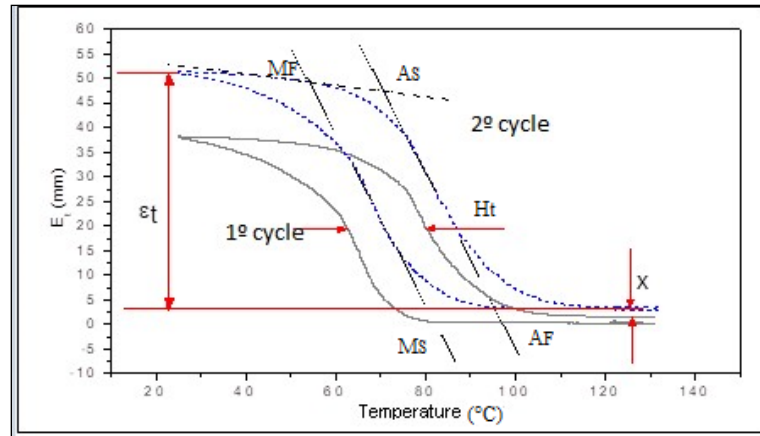


Fig. 2: Representative thermoelastic deformation versus temperature curves obtained during a typical test of thermomechanical cycles in simple bending mode. The investigated parameters are pointed out in this figure [25]. “Reproduced with permission from Gonzalez, C.H. and De Araújo, C.J, Study of Martensitic Stabilization Under Stress in Cu–Al–Be Shape Memory Alloy Single Crystal; published by Materials Science and Engineering, 2004”.

3. RESULTS AND DISCUSSIONS

3.1 Calorimetric Curves (DSC)

Figures 3-6 show calorimetric curves for the samples submitted to the five conditions: homogenized (H), rolled (RL), rolled and annealed (RA), and extruded (E), respectively.

Figure 3 was used as the reference sample. In the case of the rolled sample (RL) (Fig. 4), the start temperature of the R-phase remains practically unchanged from to M_s temperature of the homogenized (H) sample (Fig. 3). The curve of the rolled sample (Fig. 4) indicates that the plastic deformation process causes a decrease in M_s temperature during cooling and A_s temperature is also reduced. In principle, it can be assumed that the initial inflection during cooling is due to the presence of the rhombohedral phase (R-phase) [1]. The plastic deformation process increases the linear defects density (dislocations) that may hinder or even inhibit direct (austenite \Rightarrow martensite) and reverses (martensite \Rightarrow austenite) martensitic transformations.

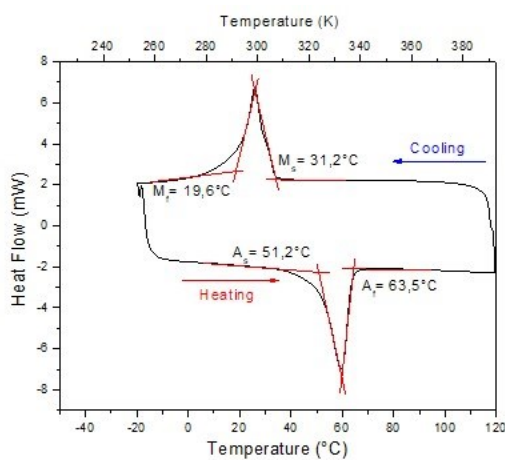


Fig. 3: Calorimetric curves with martensitic transformations of the Ni-Ti alloy homogenized (H).

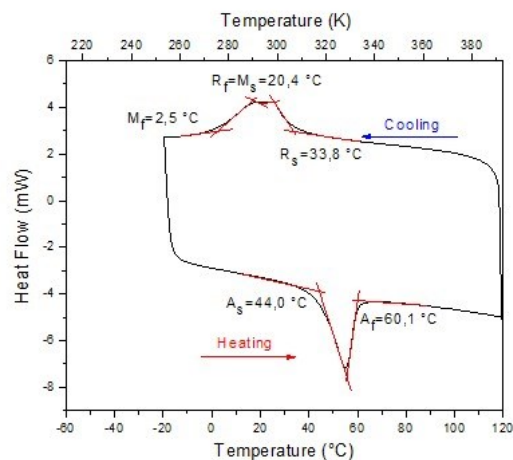


Fig. 4: Calorimetric curves with martensitic transformations of the Ni-Ti alloy rolled (RL).

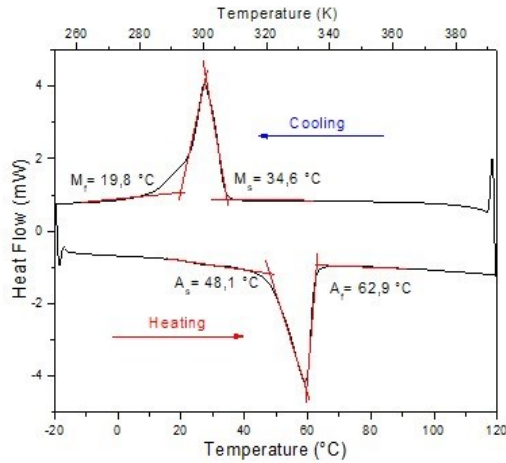


Fig. 5: Calorimetric curves with martensitic transformations of the Ni-Ti alloy rolled and annealed (RA).

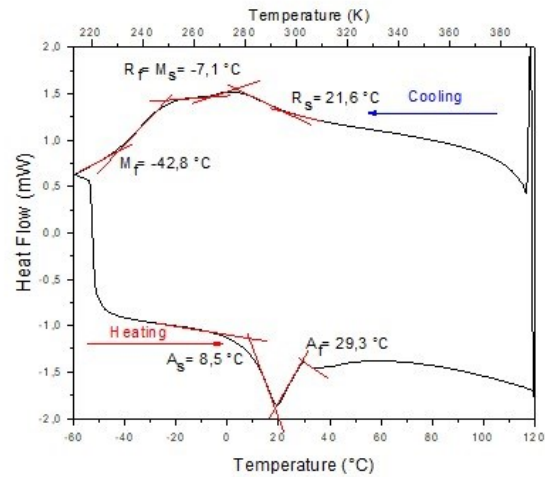


Fig. 6: Calorimetric curves with martensitic transformations of the Ni-Ti alloy extruded (E).

In the rolled and annealed (RA) sample (Fig. 5), it was observed that the calorimetric curve and its data are like the reference sample (Fig. 3), so this treatment eliminates the effects of the mechanical rolling process in this alloy.

The extruded (E) sample's (Fig. 6) DSC shows the peaks of the R-phase (rhombohedral) and monoclinic martensite phase (B19'), with lower temperatures of R_s and M_s than in the roller (RL) sample (Fig. 4). This clearly shows that the angular extrusion process introduces crystalline defects much larger than rolled process, however, it produces no reduction in the geometric dimensions of the sample.

Table 2 summarizes the main results obtained through the DSC test, the temperatures of the martensitic transformations, including the R-phase, the heating and cooling enthalpies, and the thermal hysteresis reaction.

Table 2: Martensitic transformations, enthalpies, and hysteresis of the Ni-Ti alloy samples

Sample	A_s [°C]	A_f [°C]	$\Delta H_{\text{Heating}}$ [J/g]	R_s [°C]	R_f [°C]	M_s [°C]	M_f [°C]	$\Delta H_{\text{Cooling}}$ [J/g]	H_T [°C]
H	51.2	63.5	10.3	-	-	31.2	19.6	10.9	32.3
RL	44.0	60.1	13.4	33.8	20.4	20.4	2.5	14.7	39.7
RA	48.1	62.9	15.0	-	-	34.6	19.8	13.4	28.3
E	8.5	29.3	17.2	21.6	-7.1	-7.1	-42.8	18.2	36.4
EA	26.8	42.4	17.0	31.3	14.0	-15.4	-35.5	16.0	57.8

In Fig. 7 the calorimetric curve of the extruded and annealed sample (EA) shows a complete separation between the peaks of the R-phase and the martensitic phase, with a larger temperature interval between peaks. This heat treatment was able to restore the R_s temperature of the R-phase, in this way, it was effective to eliminate (or minimize) the effects of the angular extrusion process in this crystal structure. For the martensitic phase, this treatment has become ineffective or even complicates the process to initiate the transformation.

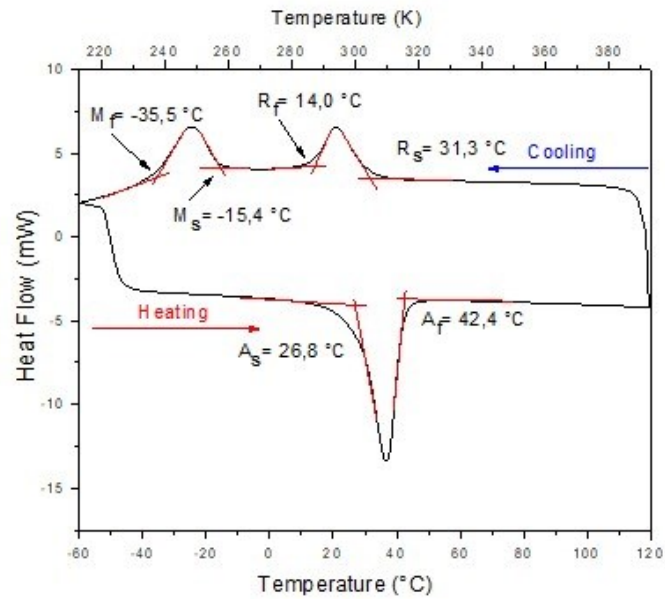


Fig. 7: Calorimetric curves with martensitic transformations of the Ni-Ti alloy extruded and annealed (EA).

3.2 Thermomechanical Test

Figures 8-12 show the thermomechanical cycling curves of the Ni-Ti samples in the bending tests under constant load. Table 3 summarizes the results obtained in these tests.

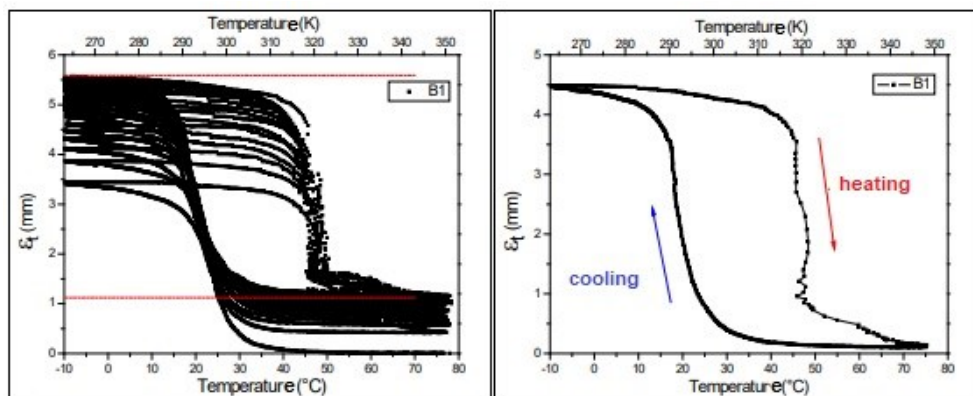


Fig. 8: Thermomechanical cycling curves of the Ni-Ti alloy homogenized (H).

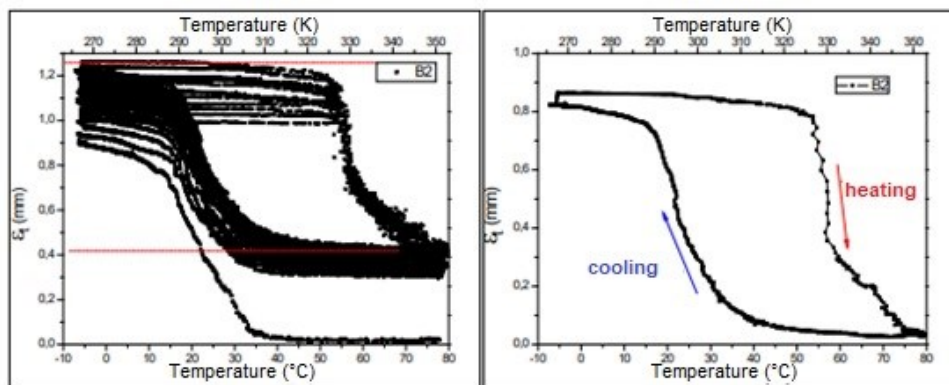


Fig. 9: Thermomechanical cycling curves of the Ni-Ti alloy rolled (RL).

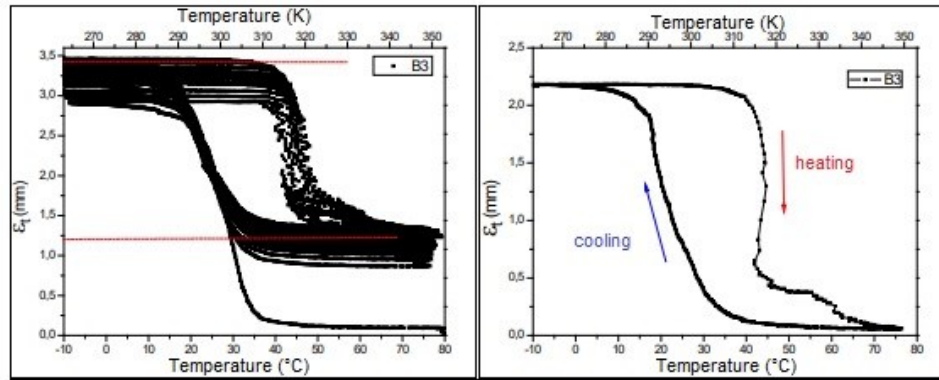


Fig. 10: Thermomechanical cycling curves of the Ni-Ti alloy rolled and annealed (RA).

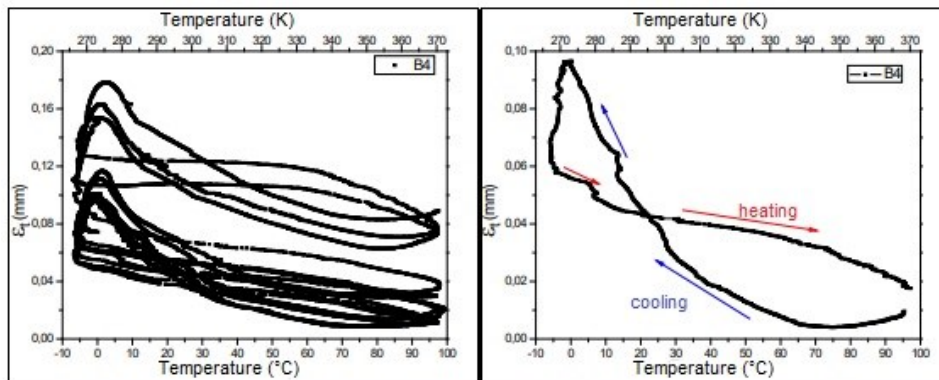


Fig. 11: Thermomechanical cycling curves of the Ni-Ti alloy extruded and annealed (EA).

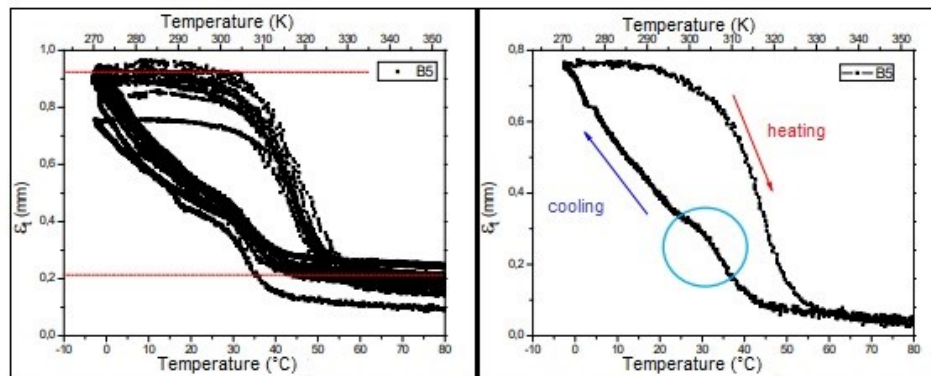


Fig. 12: Thermomechanical cycling curves of the Ni-Ti alloy in the extruded (E) condition.

Table 3: Results of the thermomechanical cycling curves of the Ni-Ti samples

Sample	A _s [°C]	A _F [°C]	R _s [°C]	R _F = M _s [°C]	M _F [°C]	ε _T [mm]
H	44.9	49.8	-	26.5	15.1	4.50
RL	53.2	74.6	-	33.2	12.6	0.86
RA	42.9	50.2	-	30.9	15.1	2.21
E	-	-	-	-	-	0.09
EA	33.2	50.8	41.7	29.1	-2.6	0.74

In Fig. 8, the homogenized (H) sample had the maximum reversible thermoelastic deformation. In the calorimetric tests, the critical temperatures of phase transformation of the rolled and annealed (RA) sample (Fig. 10) returned to effectively the same temperatures

obtained for the reference sample (H), as seen in Table 2, which also shows the enthalpies of transformation. However, this treatment was not enough to restore the reversible thermoelastic deformation obtained in the reference sample, since the maximum value obtained for the annealed sample was lower than the reference sample (H). From the results of thermoelastic tests, this treatment appears to have not been able to eliminate all the effects of the rolling process.

The extruded (E) sample (Fig. 11) practically did not show any thermoelastic deformation. This was probably due to the limitation of the thermal bath, which has a minimum temperature of -10°C, but in these cases (Fig. 12) it is also possible that the energy provided by the system was not enough to complete the entire transformation due to the blocking provided by the large increase in dislocation density. When external stress is applied to a shape memory alloy it promotes the increase of the critical transformation temperatures. The load applied was not enough for these temperatures to increase sufficiently to be detected by the device. The extruded and annealed (EA) sample (Fig. 12) showed a low recovery deformation, indicating a high degree of hardening when compared with the reference sample (H).

The heat treatment and training process seriously affects the internal friction behavior in Ti-Ni alloys. These events have an importance on the reconfiguration of Ti-Ni alloy defects, inducing modification that might change the material properties such as memory effect, damping capacity, strength, hardness, and others [26-28].

3.3 DMA Analysis

Figure 13 shows the damping curves, during heating, provided by the dynamic tests. It can be noticed that the decrease in the energy absorption capacity of the shaped samples, especially in the sample that was submitted to the ECAE, sample (E). The mechanical rolling process generates elongated grains according to the deformation direction [29,30]. These elongated grains are in a preferential direction and the result of this is the improvement of the damping capacity for RL and RA samples. The random grains obtained in sample E induce more stress field dislocation blocking the phase transformation. The large damping capacity of the EA sample is due to heat treatment who is efficient to liberate blocking regions and dislocations.

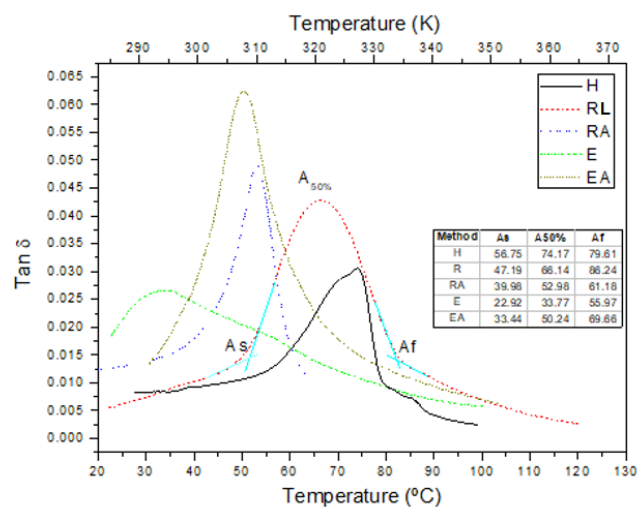


Fig. 13: DMA analysis. Temperature versus damping capacity in the conditions: homogenized (H), rolled (RL), rolled and annealed (RA), extruded (E), and extruded and annealed (EA).

According to the literature, Ni-Ti-based alloys have a high damping capacity during phase transformation and in the martensitic phase, whereas their austenitic phase shows a much lower energy dissipation [31]. The high damping capacity of the martensite phase is related to the hysteretic movement of interfaces (martensite variant interface and twin boundaries) [32,33]. It is established that the global internal friction is also controlled by dislocations and their interactions with other lattice defects. The high damping capacity of Ti-Ni alloys comes from the movement of several twin boundaries. The accommodation of twin boundaries under external stress is believed to be responsible for high damping capacity [34].

3.4 Micrography Analysis (SEM)

Figures 14-15 show micrographs of the samples. Figure 14a exhibits the microstructure of the homogenized sample and consists of equiaxial and heterogeneous grains with segregation as found in Jiang's et al. [35] work. Furthermore, as they exhibit a eutectic structure around grain boundaries, it was verified the regions with the highest percentage of Ni due to the exclusion of this element during solidification, confirmed by EDS [24].

Figure 14b and 14c show the rolled (RL) and the rolled and annealed (RA) samples. The arrows indicate this preferential orientation of the grains, which became more evident after the annealing heat treatment was carried out (Fig. 14c). Literature also suggests that with rolled process some particles of Ti_2Ni and others might be found in the grain boundaries provoking a second transformation in the grain boundaries and it is also related to R-phase transformation [36,37].

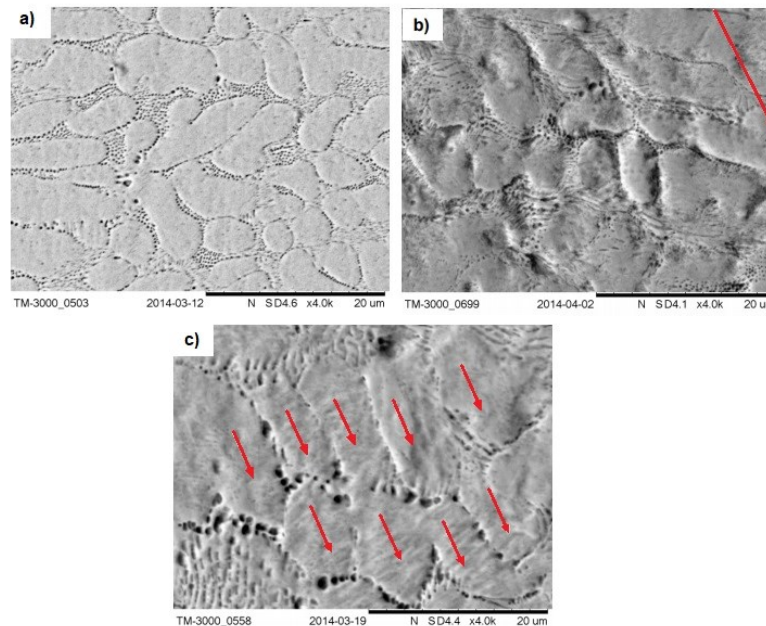


Fig. 14: SEM micrographs of samples: (a) homogenized (H), (b) rolled (RL) and (c) rolled and annealed (RA).

Figure 15 shows the microstructure for extruded (E) and extruded and annealed (EA) samples. In the images, it is possible to see the reduced grain compared with the homogenized (H) sample and particles provided by the high-stress state made by the mechanical process. These samples were subjected to severe shear deformations during the forming process, which can be confirmed by the reduction of transformation temperatures, damping capacity, and thermoelastic deformation. From the images, despite not having a

morphology with preferential orientation, it is possible to visualize the contours and decrease the grain sizes of the homogenized (H) sample. There is the presence of particles between the grains, which suggests that they are precipitated from the state of tension caused by ECAE.

Unlike samples annealed after conventional rolling, the micrographs of rolled and extruded (Fig. 15b) samples show that the latter process produces grains without preferential orientation. Probably, the configuration of the stress fields generated by the increased dislocation density must be highly disoriented. These facts seem to be responsible for the greatest loss of thermoelastic properties in the extruded samples.

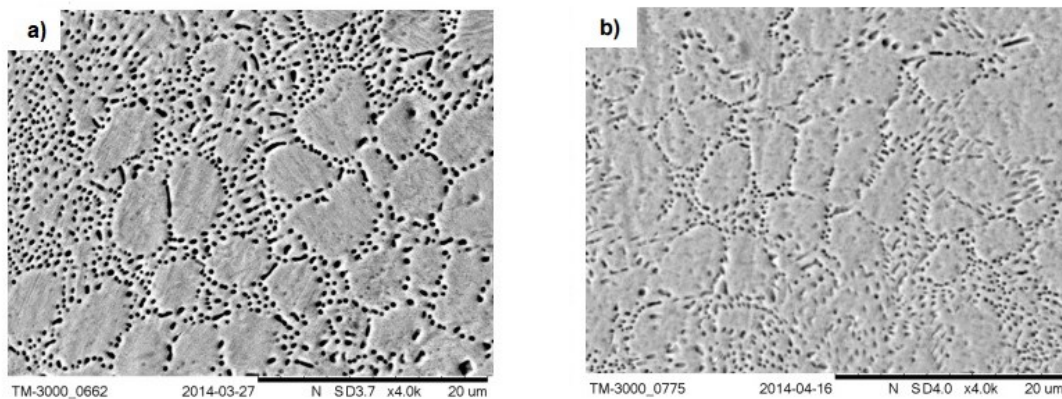


Fig. 15: SEM micrographs of samples: a) extruded (E) and b) extruded and annealed (EA).

3.5 Energy Dispersive Spectroscopy (EDS)

Figure 16 shows the analyzed regions of the sample as cast, where the percentage of elements in the alloy matrix (A), inside the grain (B), and in the region of its contour (C) was verified.

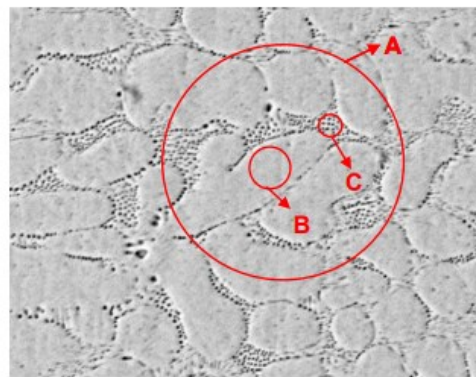


Fig. 16. EDS' analyzed regions: alloy matrix (A), inside the grain (B), and in the region of its contour (C).

Figures 17, 18, and 19 showed results of each region introduced in Fig. 16. The percentage in weight is close to the nominal of the alloy, considering it to be a semi-quantitative analysis with a certain margin of error (around 5%). In turn, it was revealed the presence of a high percentage of nickel in the region along the grain boundaries, a probable result of the precipitation of this element during the solidification of the Ni-Ti alloys [38].

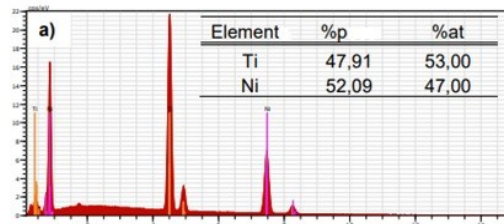


Fig. 17: EDS of area A showed in Fig. 16.

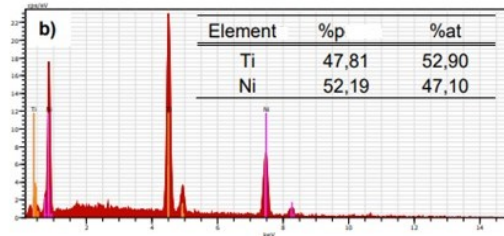


Fig. 18: EDS of area B showed in Fig. 16.

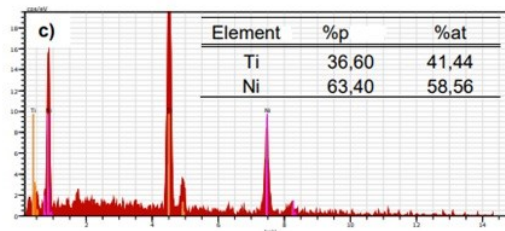


Fig. 19: EDS of area C showed in Fig. 16.

An EDS analysis for the equiatomic alloy showed a higher amount of Ni in the grain boundary region. Although the percentage of Ti is still lower, there is an increase in the detection of this element compared to the homogenized (H) sample, which suggests the presence of precipitates related to the mechanical conformation, Ti_2Ni .

4. CONCLUSION

Plastic forming processes by mechanical rolling and angular extrusion promoted increased mechanical resistance of samples due to the reduction of the grain size caused by shear stress during plastic deformation and introducing defects in the crystalline structure. Mechanical rolling and angular extrusion increased the mechanical resistance of samples by reducing the grain size and introducing defects in the crystalline structure. These processes have significantly affected the thermoelastic behavior of the shape memory alloy. Although one cannot compare directly (quantitatively) the influence of the two processes on the properties of shape memory alloys, it became evident that the process of angular extrusion seems to be much more effective in hardening the samples.

The results of the calorimetry curves when compared with data curves under constant load tests are complementary. The critical phase transformation temperatures of the samples were reduced by plastic deformation processes since there is a higher need for energy to perform the transformations.

The micrographs of rolled and extruded samples show that the latter process produces grains without preferential orientation. Probably, the configuration of the stress fields

generated by the increased dislocation density must be highly disoriented. These facts seem to be responsible for the greatest loss of thermoelastic properties in the extruded samples.

In the technological applications of the SMA, it is important to take into consideration the fact that the increased mechanical strength is achieved at the expense of reduced transformation temperatures and of the thermoelastic properties of the shape memory effect and may be recovered partly by heat treatment.

The extrusion-forming process proved to be more severe than the rolling process to the shape-recovery properties presented by the alloys. This analysis is of great importance in the use of LMF in applications that require high mechanical strength combined with the functional properties of shape recovery provided by martensitic phase transformations.

ACKNOWLEDGEMENT

This work was supported by the Conselho Nacional de Desenvolvimento Científico e Tecnológico (CNPq); Coordenação de Aperfeiçoamento de Pessoal de Nível Superior (CAPES) and the Fundação de Amparo à Ciência e Tecnologia do Estado de Pernambuco (FACEPE).

REFERENCES

- [1] Otsuka K, Wayman CM. (1998) Shape Memory Materials. Cambridge, Cambridge University Press.
- [2] Qader IN, Kök M, Dagdelen F, Abdullah SS. (2020) The effect of different parameters on shape memory alloys. *Sakarya University Journal of Science*, 24(5): 881-902. doi: 10.16984/saufenbilder.733645
- [3] DesRoches R, McCormick J, Delemont M. (2004) Cyclic properties of superelastic shape memory alloy wires and bars. *Journal of Structural Engineering*, 130(1): 38-46. doi:10.1061/(ASCE)0733-9445(2004)130:1(38)
- [4] Antunes AS, Tosetti JPV, Otubo J. (2013) High shape recovery Ni–Ti SMA wire produced from electron beam melted ingot. *Journal of Alloys and Compounds*, 577(1): 265-267. doi:10.1016/j.jallcom.2012.03.043
- [5] De Araújo CJ, Gomes AAC, Silva JA, Cavalcanti AJT, Reis RPB, Gonzalez CH. (2009) Fabrication of shape memory alloys using the plasma skull push-pull process. *Journal of Materials Processing Technology*, 209(7): 3657-3664. doi:10.1016/j.jmatprotec.2008.08.025
- [6] Silva NJ. (2018) Estudo de ligas com memória de forma Ni-Ti processadas por laminação e extrusão angular. PhD thesis. Universidade Federal de Pernambuco, Centro de Tecnologia e Geociências.
- [7] Silva KCA. (2014) Estudo de ligas com memória de forma Ni-Ti processadas por laminação e extrusão angular. PhD thesis. Universidade Federal de Pernambuco, Centro de Tecnologia e Geociências.
- [8] Figueiredo AM, Modenesi P, Buono V. (2009) Low-cycle fatigue life of superelastic NiTi wires. *International Journal of Fatigue*, 31(4): 751-758. doi:10.1016/j.ijfatigue.2008.03.014
- [9] Segal VM. (1995) Materials processing by simple shear. *Materials Science and Engineering: A*, 197(2):157-164. doi:10.1016/0921-5093(95)09705-8
- [10] Sun X, Wu DY, Kang M, Ramesh KT, Kecskes LJ. (2023) Properties and hardening behavior of equal channel angular extrusion processed Mg-Al binary alloys. *Materials Characterization*, 195: 112514. doi:10.1016/j.matchar.2022.112514
- [11] Yang Z, Li H, Zhang Y, Liu X, Gu Q, Liu X. (2022) ECAP based regulation mechanism of shape memory properties of NiTiNb alloys. *Journal of Alloys and Compounds*, 897: 163184. doi:10.1016/j.jallcom.2021.163184

- [12] Leitner T, Sabirov I, Pippan R, Hohenwarter A. (2017) The effect of severe grain refinement on the damage tolerance of a superelastic NiTi shape memory alloy. *Journal of the Mechanical Behavior of Biomedical Materials*, 71:337-348. doi:10.1016/j.jmbbm.2017.03.020
- [13] Jiang SY, Yu JB, Zhang YQ, Xing XD. (2020) Mechanically-induced martensite transformation of NiTiFe shape memory alloy subjected to plane strain compression. *Trans. Nonferrous Met. Soc. China*, 30: 1325-1334. doi:10.1016/S1003-6326(20)65299-2
- [14] Zhang J, Chen T, Li W, Bednarcik J, Dippel AC. (2020) High temperature superelasticity realized in equiatomic Ti-Ni conventional shape memory alloy by severe cold rolling. *Materials and Design*, 193: 1008875. doi:10.1016/j.matdes.2020.108875
- [15] Liang Q, Zhao S, Liang C, Zhao T, Wang D, Ding X, Li S, Wang Y, Zheng Y, Ren X, Mills M, Wang Y. (2022) Strain states and unique properties in cold-rolled TiNi shape memory alloys. *Acta Materialia*, 231: 117890, 2022. doi:10.1016/j.actamat.2022.117890
- [16] Silva TTL. (2022) Comportamento termoeástico de fios de Ni-Ti com efeito memória de forma processados por laminação a frio. PhD thesis. Universidade Federal de Pernambuco, Centro de Tecnologia e Geociências.
- [17] Silva TTL, Virgolino FSS, Oliveira CAN, de Araújo CJ, Gonzalez CH. (2021) Fabricação de uma liga equiatômica de TiNi com efeito memória de forma pelo método plasma skul-push pull. *Revista Engenharia e Tecnologia*, 13(4): 270-280. Retrieved from <https://revistas.uepg.br/index.php/ret/article/view/19659>
- [18] Simões JB. (2017) Fabricação de componentes miniaturizados de ligas com memória de forma NITI usando fundição de precisão. João Pessoa, Ideia.
- [19] Virgolino FSS. (2017) Comportamento em fadiga termomecânica de fios de liga com memória de forma Ni-Ti-Cu. Dissertation. Universidade Federal de Pernambuco, Centro de Tecnologia e Geociência.
- [20] Aghamiri SMS, Ahmadabadi MN, Shahmir H, Naghdi F, Raygan S. (2013) Study of thermomechanical treatment on mechanical-induced phase transformation of NiTi and TiNiCu wires. *Journal of the mechanical behavior of biomedical materials*, 21: 32-36. doi:10.1016/j.jmbbm.2013.01.014
- [21] Karaca HE, Kaya I, Tobe H, Basaran B, Nagasako M, Kainuma R, Chumlyakov S. (2013) Shape memory behavior of high strength Ni₅₄Ti₄₆ alloys. *Materials Science & Engineering*, 580: 66-70. doi:10.1016/j.msea.2013.04.102
- [22] Khaleghi F, Allafi JK, Chianeh VA, Noori S. (2013) Effect of short-time annealing treatment on the superelastic behavior of cold drawn Ni-rich NiTi shape memory wires. *Journal of Alloys and Compounds*, 554: 32-38. doi:10.1016/j.jallcom.2012.11.183
- [23] Van Humbeeck J. (2003) Damping capacity of thermoelastic martensite in shape memory alloys. *Journal of Alloys and Compounds*, 335(1-2): 58-64. doi:10.1016/S0925-8388(03)00268-8
- [24] Oliveira CAN, Gonzalez CH, De Araújo CJ, Araujo Filho OO, Urtiga Filho SUL. (2010) Thermoelastic Properties on Cu-Zn-Al Shape Memory Springs. *Materials Research*, 13(2): 219-223. doi:10.1590/S1516-14392010000200016
- [25] Gonzalez CH, De Araújo CJ, Quadros NF, Guénin G, Morin M. (2004) Study of Martensitic Stabilization Under Stress in Cu-Al-Be Shape Memory Alloy Single Crystal. *Materials Science and Engineering*, 378(1-2): 253-256. doi:10.1016/j.msea.2003.11.069
- [26] Yoshida I, Ono T, Asai M. (2000) Internal friction of Ti-Ni alloys. *Journal of Alloys and Compounds*, 310(1-2):339-343. doi:10.1016/S0925-8388(00)00957-9
- [27] Yoshida I, Monma D, Iino K, Ono T, Otsuka K, Asai M. (2004) Internal friction of Ti-Ni-Cu ternary shape memory alloys, *Mat Sci. Engineering Structures*, 370(1-2): 444-448. doi:10.1016/j.msea.2003.05.003
- [28] Genlian Fan YZ, Otsuka K, Ren X. (2006) Ultrahigh damping in R-phase state of Ti-Ni-Fe alloy. *Applied Physics Letters*, 89:3. doi:10.1063/1.2363173
- [29] Ma Y, Du Z, Cui X, Cheng J, Liu G, Gong T. et al. (2018) Effect of cold rolling process on microstructure and mechanical properties of high strength β titanium alloy thin sheets. *Progress in Natural Science: Materials International*, 28(6): 711-717. doi:10.1016/j.pnsc.2018.10.004

- [30] Sadeghpour S, Abbasi SM, Morakabati M, Karjalainen LP, Porter DA. (2018) Effect of cold rolling and subsequent annealing on grain refinement of a beta titanium alloy showing stress-induced martensitic transformation. *Materials Science and Engineering: A*, 731: 465-478. doi:10.1016/j.msea.2018.06.050
- [31] Lu XL, Cai W, Zhao LC. (2003) Damping behavior of a Ti44Ni47Nb9 shape memory alloy. *Journal of Materials Science Letters*, 22: 1243-1245. doi:10.1023/A:1025445832316
- [32] Van Humbeeck J, Liu Y (2000). *The High Damping Capacity of Shape Memory Alloys*. Springer-Verlag. https://doi.org/10.1007/978-3-642-59768-8_4
- [33] Oliveira CAN, Gonzalez CH, Araujo Filho OO, Silva NJ, Guimaraes PB, Mendonza EN et al. (2015) Thermomechanical Analysis on Ti-Ni Shape Memory Helical Springs Under Cyclic Tensile Loads. *Mat. Res.*, 18(2): 17-24. doi:10.1590/1516-1439.334514
- [34] Wu SK, Lin HC. (2003) Damping characteristics of TiNi binary and ternary shape memory alloys. *Journal of alloys and compounds*, 355(1-2): 72-78. doi:10.1016/S0925-8388(03)00279-2
- [35] Jiang SY, Zhang YQ. (2012) Microstructure evolution and deformation behavior of as-cast Ni-Ti shape memory alloy under compression. *Transactions of Nonferrous Metals Society of China*, 22(1): 90-96. doi:10.1016/S1003-6326(11)61145-X
- [36] Bhagyaraj J, Ramaiah KV, Saikrishna CN, Bhaumik SK, Gouthama. (2013) Behavior and effect of Ti2Ni phase during processing of Ni-Ti shape memory alloy wire from cast ingot. *Journal of Alloys and Compounds*, 581: 344-351. doi:10.1016/j.jallcom.2013.07.046
- [37] Duerig TW, Bhattacharya K. (2015) The Influence of the R-Phase on the Superelastic Behavior of NiTi. *Shape Memory and Superelasticity*, 1: 153-161. doi:10.1007/s40830-015-0013-4
- [38] Chen Y, Jiang HC, Liu SW, Rong LJ, Zhao XQ. (2009) Damping capacity of TiNi-based shape memory alloys. *Journal of Alloys and Compounds*, 482(1-2): 151-154. doi:10.1016/j.jallcom.2009.03.148